

A DFT study of structural, dynamical properties and quasiparticle band structure of solid nitromethane

S. Appalakondaiah and G. Vaitheeswaran*

*Advanced Centre of Research in High Energy Materials (ACRHEM),
University of Hyderabad, Prof. C. R. Rao Road,
Gachibowli, Andhra Pradesh, Hyderabad- 500 046, India.*

S. Lebègue

*Laboratoire de Cristallographie, Résonance Magnétique et Modélisations (CRM2,
UMR CNRS 7036), Institut Jean Barriol, Université de Lorraine, BP 239,
Boulevard des Aiguillettes, 54506 Vandoeuvre-lès-Nancy, France.*

(Dated: September 23, 2018)

We report a detailed theoretical study of the structural, vibrational, and optical properties of solid nitromethane using first principles density functional calculations. The ground state properties were calculated using a plane wave pseudopotential code with either the local density approximation (LDA), the generalized gradient approximation (GGA), or with a correction to include van der Waals interactions. Our calculated equilibrium lattice parameters and volume using a dispersion correction are found to be in reasonable agreement with the experimental results. Also, our calculations reproduce the experimental trends in the structural properties at high pressure. It was found to be a discontinuity in the bond length, bond angles and also a weakening of hydrogen bond strength in the pressure range from 10 to 12 GPa, picturing the structural transition from phase I to Phase II. Moreover, we predict the elastic constants of solid nitromethane and found that the corresponding bulk modulus is in good agreement with experiments. The calculated elastic constants are showing an order of $C_{11} > C_{22} > C_{33}$, indicating that the material is more compressible along the c-axis. We also calculated the zone center vibrational frequencies and discuss the internal and external modes of this material under pressure. From this, we found the softening of lattice modes around 8 to 12 GPa. We have also attempted the quasiparticle band structure of solid nitromethane with the G_0W_0 approximation and found that nitromethane is an indirect band gap insulator with a value of the band gap of about 7.8 eV with G_0W_0 approximation. Finally, the optical properties of this material, namely the absorptive and dispersive part of the dielectric function, and the refractive index and absorption spectra are calculated and the contribution of different transition peaks of the absorption spectra are analyzed. The static dielectric constant and refractive indices along the three inequivalent crystallographic directions indicate that this material has a considerable optical anisotropy.

PACS numbers:

I. INTRODUCTION

Nitromethane is one of the simplest organic compounds which belong to the class of secondary explosives. It is insensitive, safe to handle, used as a storable monopropellant and as an additive fuel for combustion engines. Because of its simple crystal structure compared with other secondary explosives, it has been used as a prototype material to understand the energetic materials by both experimentalists¹⁻¹⁰ and theoreticians.¹¹⁻¹⁷ Nitromethane is liquid at room temperature but the molecules condense to form a solid at around 4.2 K. Trivero et al.¹ first reported X-rays and neutron diffraction experiments, and found that solid nitromethane crystallizes in an orthorhombic structure in the space group $P2_12_12_1$. Also, several experimental studies have been reported on the structural³⁻⁵ and the dynamical⁶⁻¹⁰ properties of nitromethane at various pressures and temperatures. A considerable amount of theoretical work has been performed using classical and quantum molecular dynamics simulations under various conditions.^{11,12,18-20}

By using classical interatomic potential molecular dynamics simulations, Sorescu et al.¹¹ predicted the structural properties of nitromethane crystals. The thermal decomposition of nitromethane was investigated using Car-Parrinello molecular dynamics simulations, which reveals that it undergoes a thermal decomposition at 2200 K with the cleavage of the C-N bonds.²¹ The anisotropic nature of solid nitromethane was studied using pseudopotential approach by applying hydrostatic pressure up to 20 GPa.¹⁶ Recently, Sorescu et al.²² and Landerville et al.²³ reported the structural properties of nitromethane using respectively the parametrization of Grimme²⁴ and of Neumann and Perrin.²⁵

Accurate and reliable calculations of electronic properties of secondary explosive materials with standard Density Functional Theory (DFT) are a difficult and challenging issue due to their complex crystal structure mainly controlled by van der Waals interactions. Also, the electronic band gap plays a major role in determining the impact sensitivity and detonation or defragmentation properties of explosive materials. It is well known that stan-

standard DFT using exchange-correlational functionals like the local density approximation (LDA) or the generalized gradient approximation (GGA) always underestimate the band gap by about 30 - 40%,^{27,28} therefore one has to use for instance the GW approximation to know the exact band gap value accurately.^{29,30} In the present study, efforts are taken to understand the structural and dynamical properties of solid nitromethane at zero and high pressures including van der Waals interaction. We also predict the elastic constants of this material to explore the stability and detonation characteristics. In addition to these calculations, quasiparticle band structure using the GW approximation and thereby the optical properties of the solid nitromethane are studied. The rest of the paper is organized as follows: in section II, we briefly describe the computational techniques while the results and discussions are presented in section III. Finally, a brief conclusion is given in section IV.

II. COMPUTATIONAL DETAILS

The ground state properties are obtained using DFT in the Kohn-Sham formalism³² as implemented in the CASTEP simulation package^{33,34}. The Kohn-Sham orbitals of the valence electrons are expressed in a plane wave basis set and ultrasoft pseudopotentials are used to describe the electron-nuclei interactions. The LDA³⁶ as well as the GGA schemes of Perdew and Wang³⁷ (PW91) and of Perdew-Burke-Ernzerhof³⁸ (PBE) for the treatment of the exchange and correlation are used. Structural optimizations were performed by minimizing the forces on each atom until they were lower than $0.03 \text{ eV}\text{\AA}^{-1}$. A plane wave kinetic energy cutoff of 620 eV was used and the Brillouin zone was sampled on a regular Monkhorst-Pack³⁹ grid of $6 \times 5 \times 4$ points with a minimum spacing of 0.025 \AA^{-1} . The pseudopotentials were considered according to Vanderbilt's ultrasoft⁴⁰ scheme with a number of valence electrons of 1 for hydrogen, 4 for carbon, 5 for nitrogen, and 6 for oxygen. To take into account vdW interactions which are often present in molecular crystals, we have used various DFT-D methods as implemented in CASTEP. In the case of DFT-D calculations, the total energies of the system can be expressed as $E_{DFT-D} = E_{DFT} + E_{dispersion}$, where E_{DFT} is the self consistent Kohn-Sham energy and $E_{dispersion}$ is written as $f(R_{ij}) \times C_6^{ij} \times R_{ij}^{-6}$ for each pair (ij) of atoms separated by a distance R_{ij} . $f(R)$ is a damping function which is necessary to avoid divergence for small values of R , and C_6^{ij} is the dispersion coefficient for the atom pair (ij) . In the present work, different DFT-D approaches to treat vdW interactions were employed, notably the Ortmann, Bechstedt and Schmidt⁴¹ (OBS) correction to PW91, as well as the Tkatchenko and Scheffler⁴² (TS) and Grimme (G06)²⁴ corrections to PBE.

In order to overcome the difficulties in density functional theory within standard functionals like the LDA or the GGA to calculate excited states, including the

band gap which is underestimated, we have used the GW approximation^{44,45} to obtain the bandstructure of solid nitromethane. Instead of the Kohn-Sham equations used in DFT, the following quasiparticle equation is solved:

$$(T + V_{ext} + V_h)\psi_{\mathbf{k}n}(\mathbf{r}) + \int d^3r' \Sigma(\mathbf{r}, \mathbf{r}', E_n(\mathbf{k}))\psi_{\mathbf{k}n}(\mathbf{r}') \quad (1)$$

$$= E_n(\mathbf{k})\psi_{\mathbf{k}n}(\mathbf{r})$$

where T is the kinetic energy operator, V_{ext} is the external potential from the ion cores, V_h is the Hartree potential, Σ is the self-energy operator, and $E_n(\mathbf{k})$ and $\psi_{\mathbf{k}n}(\mathbf{r})$ are respectively the quasiparticle energy and the quasiparticle wave function. Then, Σ is approximated (vertex corrections are neglected) as the product of the Green's function G times the screened Coulomb interaction W , which gives the GW approximation. In practice, the GW quasiparticle eigenvalues are calculated as a correction to the DFT eigenvalues $\epsilon_n(\mathbf{k})$ like⁴⁸:

$$\text{Re } E_n(\mathbf{k}) = \epsilon_n^{DFT}(\mathbf{k}) + Z_{n\mathbf{k}} \quad (2)$$

$$\times [\langle \Psi_{\mathbf{k}n}^{DFT} | \text{Re} \Sigma(\mathbf{r}, \mathbf{r}', \epsilon_n(\mathbf{k})) | \Psi_{\mathbf{k}n}^{DFT} \rangle$$

$$- \langle \Psi_{\mathbf{k}n}^{DFT} | V_{xc}^{DFT}(r) | \Psi_{\mathbf{k}n}^{DFT} \rangle]$$

with the QP renormalization factor $Z_{n\mathbf{k}}$ being:

$$Z_{n\mathbf{k}}^{DFT} = [1 - \langle \Psi_{\mathbf{k}n}^{DFT} | \frac{\partial}{\partial \omega} \text{Re} \Sigma(\mathbf{r}, \mathbf{r}', \epsilon_n(\mathbf{k})) | \Psi_{\mathbf{k}n}^{DFT} \rangle]^{-1}.$$

We have used the implementation of the G_0W_0 approximation^{29,30} provided by the code VASP (Vienna Ab-initio Simulation Package)⁴⁹. To obtain convergence, we used 200 bands for the summation over the bands in the polarizability and the self-energy formulas, and the polarizability matrices were calculated up to a cut-off of 150 eV.

III. RESULTS AND DISCUSSIONS

A. Structural properties

As the starting point of our calculations, we adopted the experimental crystal structure of solid nitromethane¹ having the $P2_12_12_1$ space group and with lattice vectors of $a = 5.183 \text{ \AA}$, $b = 6.236 \text{ \AA}$, $c = 8.518 \text{ \AA}$, which contains four molecules (28 atoms) of nitromethane per unit cell (see Fig. 1). The calculated equilibrium lattice parameters, volumes and relative deviations with experimental results are presented in Table I. We observe a large difference between our calculated values obtained with either the LDA, GGA-PBE, or GGA-PW91 functional (which are in reasonable agreement with earlier reported calculations^{16,20}) and the experimental datas. For instance, the equilibrium volume obtained with LDA (239.8 \AA^3) is much lower than the experimental value (275.3 \AA^3), while the values obtained with GGA-PW91 (339.6 \AA^3) or GGA-PBE (334.98 \AA^3) are 20 % too large.

TABLE I: The calculated ground state properties of solid nitromethane at zero pressure. a , b and c are the lattice parameters, V the volume of the orthorhombic unit cell. (in parenthesis: relative deviations from experiments (Ref. 1))

Method	XC	$a(\text{\AA})$	$b(\text{\AA})$	$c(\text{\AA})$	$V(\text{\AA}^3)$
DFT	LDA-CAPZ	4.91 (-5.3%)	6.03 (-3.3%)	8.10 (-4.9%)	239.82 (-12.9%)
	GGA-PW91	5.49 (+5.9%)	6.76 (+8.4%)	9.15 (+7.4%)	339.59 (+23.3%)
	GGA-PBE	5.47 (+5.5%)	6.73 (7.9%)	9.10 (+6.8%)	334.98 (+21.7%)
DFT-D	GGA-PW91-OBS	5.05 (-2.6%)	6.24 (0.1%)	8.44 (-0.9%)	266.43 (-3.2%)
	GGA-PBE-TS	5.21 (+0.5%)	6.48 (3.9%)	8.64 (+1.4%)	291.97 (+6.1%)
	GGA-PBE-G06	5.19 (+0.1%)	6.29 (+0.9%)	8.58 (+0.7%)	280.01 (+1.7%)
Exp ^a		5.183	6.235	8.518	275.31

a : Ref. 1 (Neutron diffraction at 4.2 K).

However solid nitromethane is a molecular crystal where intermolecular interactions are dominated by van der Waals forces, and such interactions are not described correctly by standard functionals such as LDA or GGA. To improve our results, we have used various DFT-D methods to describe vdW forces in our calculations (see table I), which show a good agreement with the experimental values. Overall, the structural properties obtained with the PBE-G06 are showing the closest agreement with experiments. and therefore we will proceed further with this functional and also with the standard functionals LDA and PBE for comparison. Notice that our results are in agreement with previous studies^{5,22,23} on solid nitromethane using similar methods.

In order to examine the effect of hydrostatic pressure on this material, we also computed the structural properties of solid nitromethane up to 30 GPa. The variation in the lattice constants a , b , and c as function of pressure are compared with experiments in Fig. 2(a). To cover the various range of pressure of 0-6 GPa³, 0-15 GPa⁴ and 0-30 GPa⁵ of the different experiments, we conduct our calculations from 0 GPa to 15 GPa with steps of 2 GPa and continue with steps of 5 GPa size up to 30 GPa. While at low pressure the +D correction to PBE is essential to reproduce the experimental values, at large pressure the three functionals give close results, which implies that at high pressures the long-range vdW forces become less important, as expected. Moreover it is seen that when using PBE-G06 functional, a sudden change in the lattice parameters occurs between 10 GPa to 12 GPa: the lattice parameters a and b decreases with increasing pressure whereas the c lattice parameter increases with pressure. A similar behavior is observed with the LDA and PBE functionals, although it happens at higher pres-

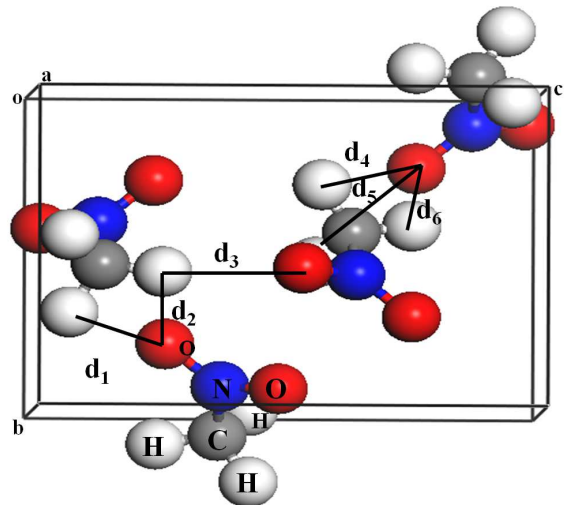


FIG. 1: (Colour online) Optimized crystal structure of solid nitromethane using GGA+G06 at 0 GPa. Here d_i ($i=1-6$) are the different O-H bonds.

sure (between 15 GPa to 20 GPa).

To understand the sudden change in the lattice parameters, we have calculated the pressure dependence of the bond lengths and of the bond angles, the corresponding data are shown in Fig. 3 and Fig. 4. The change observed in the lattice parameters is also reflected in the bond lengths and bond angles. In particular, when hydrostatic pressure is increased from 0 GPa to 10 GPa with the PBE-G06 functional, the bond lengths C-N, N-O _{i} ($i=1,2$), O-H _{i} ($i=1,6$) and the bond angle O₁-N-

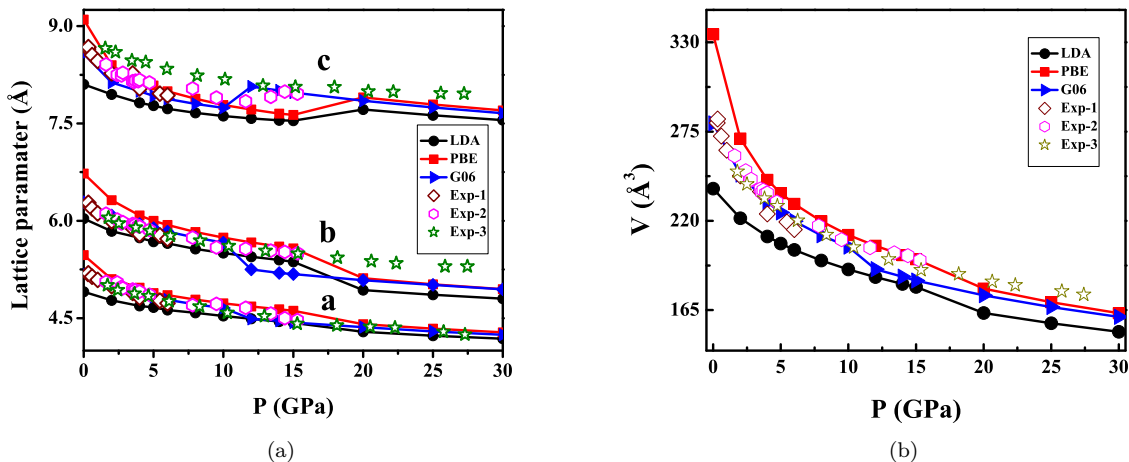


FIG. 2: (Colour online) (a). Pressure dependence of lattice parameters a, b, and c (b). Comparison of the pressure dependence of the crystal volume of solid nitromethane up to 30 GPa as calculated within LDA, PBE, and PBE-G06, compared to experiments (Exp1: Ref. 3, Exp2: Ref. 4, Exp3: Ref. 5)

O₂ decreases significantly but in contrast, the C-N-O_i (i=1,2) bond angles increases with pressure. However in the pressure region from 10 GPa to 12 GPa, an increase in the N-O₂ bond length is observed together with a sudden change in the C-N-O bond angles. Also, the O-H distances (see Fig. 4) d₁, d₃ and d₆ are in the range of 2.2 Å to 3.2 Å at zero pressure, whereas these values decreases to 2.0 Å to 2.6 Å at high pressures and we found weakening of hydrogen bond strength in 10 to 12 GPa. This behavior indicates slight changes in the hydrogen bonding and more generally in the intermolecular geometry of solid nitromethane. In Fig. 5. we have pictured the unit cell of solid nitromethane for different pressures. A phase transition is clearly observable, which corresponds to the Phase I to Phase II known experimentally⁵ to occur at 11 GPa. In our case the transition pressure is slightly different, but the overall agreement is found to be good.

Fig 2(b) shows our calculated pressure-volume relation up to 30 GPa and compared with experiments. The calculated bulk modulus and its pressure derivative obtained with the PBE-G06 functional are $B = 11.6$ GPa and $B' = 6.5$ respectively, which is in good agreement with experiments 7 GPa,³ 10.1 GPa,⁴ 9.25(±1.9) GPa⁵ and closely comparable with the reported theoretical values 5.7 GPa,¹¹ 5.7 GPa.¹⁶

B. Elastic properties

To have a better understanding of the mechanical properties of nitromethane, we have studied the corresponding elastic properties. We have used the PBE-G06 functional since it provided us with lattice parameters in close agreement with experiments (See Table I). Solid

nitromethane crystallizes in an orthorhombic structure, it has 9 independent elastic constants namely C_{11} , C_{22} , C_{33} , C_{44} , C_{55} , C_{66} , C_{12} , C_{13} and C_{23} . To calculate the elastic properties, we have used the volume-conserving strain technique⁵⁰ and the calculated single crystal elastic constants are presented in Table II.

TABLE II: Single crystal elastic constants (C_{ij} , in GPa) of solid nitromethane. All quantities are calculated at the respective theoretical equilibrium volume obtained with the GGA-G06 functional.

C_{11}	C_{22}	C_{33}	C_{44}	C_{55}	C_{66}	C_{12}	C_{13}	C_{23}
20.3	20.1	16.1	5.2	1.4	6.2	7.4	7.2	4.6

The calculated values satisfy the Born stability criteria⁵¹ for an orthorhombic structure and indicates that the system is mechanically stable. For an orthorhombic structure, the elastic constants C_{11} , C_{22} , and C_{33} are directly related to the compression of crystallographic axes along the a, b, and c axes. In the case of solid nitromethane, they follow an order of $C_{11} > C_{22} > C_{33}$ which implies that C_{11} is the stiffest elastic constant: one can expect strong interactions along the a-axis, whereas it has more sensitive to detonation along the c-axis. A similar conclusion was obtained for solid nitromethane by Conroy et al³¹ by applying uniaxial compressions along different crystallographic planes. The other diagonal elements of the elastic tensors, C_{44} , C_{55} , and C_{66} , indicate the shear elasticity applied to two dimensional regular lattices along $[1\ 0\ 0]$, $[0\ 1\ 0]$ and $[0\ 0\ 1]$. From our calculations, we found that $C_{66} > C_{44} > C_{55}$, which indicates a softer shear transformation along the $[1\ 0\ 0]$ and $[0\ 1\ 0]$ directions in solid nitromethane than along the $[0\ 0\ 1]$ direction. The off diagonal elas-

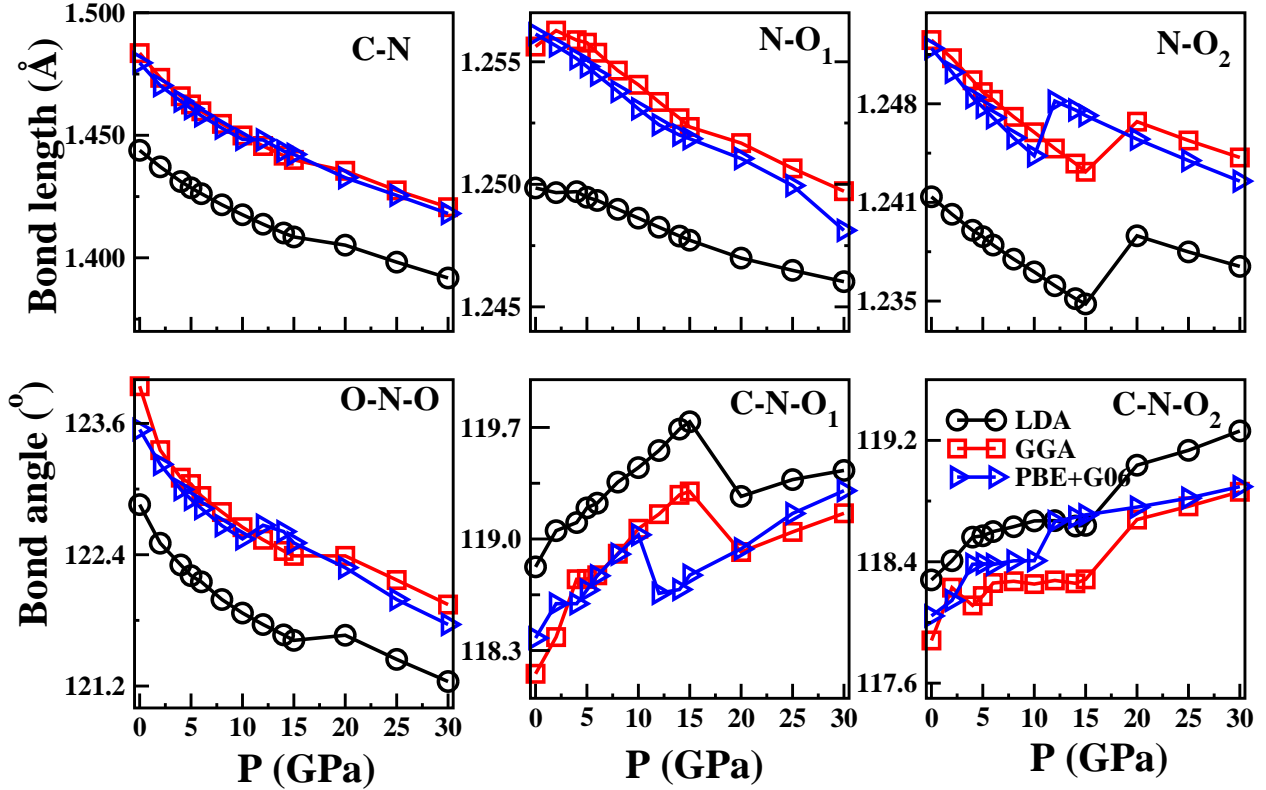


FIG. 3: (Color online) Bond lengths and bond angles of solid nitromethane up to 30 GPa as calculated within LDA, PBE, and PBE-G06.

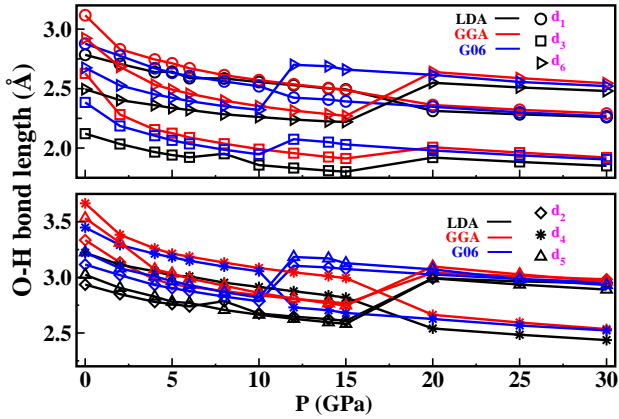


FIG. 4: (Color online) Oxygen-hydrogen bond lengths of solid nitromethane up to 30 GPa as calculated within LDA, PBE, and PBE-G06.

tic components are found to be the order of $C_{12} \geq C_{13} > C_{23}$. This implies that C_{12} and C_{13} couple an applied normal stress component in the crystallographic axis a direction with uniaxial stress along b and c axes. Though there is no experimental elastic constants available for this material, at present we compared the calculated elastic properties with other secondary explosive materials RDX,⁵² HMX⁵³ and PETN.⁵⁴ Interestingly in all these explosives, C_{11} , C_{22} and C_{33} follow the same ordering

of $C_{11} > C_{22} > C_{33}$ and this implies that most of the secondary explosives have more sensitive along crystallographic c -axis and less sensitive along a -axis. Finally the calculated single crystal bulk modulus from elastic constants is 10.32 GPa, which is excellent agreement with earlier experiments.³⁻⁵ From this, we can say that the calculated elastic constants and bulk modulus are quite reasonable.

C. Vibrational properties

In this section, we report on our investigation of the vibrational properties of solid nitromethane using linear response method with in density functional perturbation theory, as implemented in the CASTEP code. Since the unit cell of solid nitromethane contains 28 atoms, the corresponding number of modes are 84, of which 3 are acoustic modes and remaining 81 modes are optical modes. The optical modes at the Brillouin zone center (Γ point) have the following irreducible representation: $A(R)$, $B_1(R+IR)$, $B_2(R+IR)$ and $B_3(R+IR)$. Here R and IR represents the Raman active and infrared active respectively. Table III and IV provides the calculated internal and external modes for PBE+G06 calculations, with the corresponding mode assignment and compared with earlier experimental and other theoretical results. By following the previous notation, the high energy domain($>$

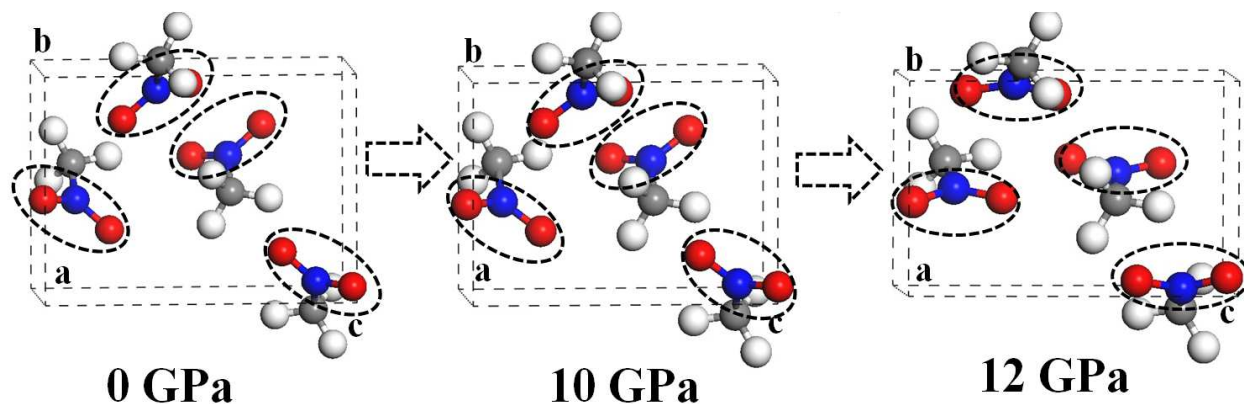


FIG. 5: (Color online) Snap shots of solid nitromethane unit cells using PBE+G06 at 0 GPa, 10 GPa and 12 GPa. The circles shows the orientation of C-N-O bond angle with pressure.

400 cm^{-1}) contains 14 internal modes where each mode grouped into four set of symmetries. These modes are indexed going from highest energy mode M1 (CH_3 antisymmetric stretching) to the lowest energy mode M14 (NO_2 rocking). The main features of the internal modes are as follows (1) The higher frequency modes M1, M2 and M3 are mainly from CH_3 stretching, (2) optical modes M5 to M8 are because of CH_3 deformation and NO_2 stretching, (3) NCH deformation is observed in mode M9, (4) mixed motions are observed in M10 to M13, which are from NO_2 , CH_3 and CN bonds (5) M14 mode is mainly from the NO_2 rocking. The calculated internal modes differ by few cm^{-1} by comparing with earlier reported GGA-PBE calculated frequencies.¹⁶ This is mainly from due to the inclusion of vdW correction to GGA which improved the volume compared by without inclusion of vdW and thereby intermolecular distance varies considerably. Whereas the low energy domain ($< 400 \text{ cm}^{-1}$) consists 25 fundamental external (lattice) modes, namely $7A+6B_1+6B_2+6B_3$. The internal and external modes are separated by 292.6 cm^{-1} , which is in good agreement with experimental gap of 289.2 cm^{-1} . Overall, the calculated external and internal modes are remarkably well in agreement with experiments.⁸⁻¹⁰

Now, we discuss the pressure dependence of the vibrational frequencies of solid nitromethane. Fig. 6 shows the frequency of the internal modes in function of pressure up to 30 GPa (with a step size of 5 GPa). It is observed that the frequencies of all the internal modes increases with external pressure. However, in the pressure range 10 GPa to 15 GPa, a large discontinuity is noticed for the vibrational modes M2, M3, M4, M7 and M8. From Table. III, it is found that the mentioned modes are from CH_3 and NO_2 stretching modes at ambient conditions and hydrostatic compression shows significant effect on CH_3 and NO_2 groups. A similar behavior has been observed from 9 to 13 GPa in the experiments using Raman

measurements⁸⁻¹⁰. The variation under pressure of lattice modes are shown in Fig. 7. From this, the calculated lattice modes from L1 to L3 (Fig. 7(a)) are hardening with increasing pressure, whereas L4 to L6 modes (Fig. 7(b)) starts softening from 5 GPa to 10 GPa. As the pressure increases from 10 GPa, all these modes (L4 to L6) shift towards higher frequencies. However in the pressure region 8 to 10 GPa, B_1 modes decreases to zero and shown in Fig. 7(c). Overall, the calculated vibrational frequencies at high pressure using PBE-G06 functional shows distinct intra and intermolecular modes at high pressures and the discontinuity in the internal and lattice modes point out to the structural transition in solid nitromethane between 10 to 12 GPa at low temperatures which is in good agreement with available experimental data.^{5,9} From 15 to 30 GPa, all the internal modes increases continuously and without any slope change, in agreement with earlier experiments. Also, by increasing the pressure the energy gap between the internal and the external modes decreases to 30 cm^{-1} , which is comparable with previous experiment.

D. Electronic properties

As mentioned earlier, in order to correlate the impact sensitivity of an explosive material with its electronic band gap, it is necessary to know the electronic band structure and the value of the band gap precisely. In particular, Wei and Xiao²⁶ correlated the impact sensitivity with the band gap of azides and confirmed that the materials having the smallest the band gap are easier to decompose and to explode under external stimuli. In the case of nitromethane, there is no experimental evidence for the value of band gap to the best of our knowledge. Our calculated bandstructure along high symmetry directions obtained with the GGA approximation is pre-

TABLE III: Vibrational frequencies (in cm^{-1}) of the internal modes of solid nitromethane. All quantities are calculated at the respective theoretical equilibrium volume using the GGA+G06 functional. Here A(R), B₁(R+IR), B₂(R+IR) and B₃(R+IR) are irreducible representation of space group P₂₁2₁2₁.

no.	Mode	Irr rep	Cal. fre	Ass.	Exp ⁸	other (PBE) ¹⁶
1		B ₁	3127.8			
2	M1	B ₂	3127.3	CH ₃ antisymmetric stretching	3082.2 (B ₂)	3117
3		B ₃	3126.5			
4		A	3126.3			
5		B ₂	3082.7			
6	M2	B ₁	3081.6	CH ₃ antisymmetric stretching	3049.6 (B ₃)	3072
7		B ₃	3081.2			
8		A	3080.9			
9		B ₂	2983.1			
10	M3	B ₁	2981.8	CH ₃ symmetric stretching		2980
11		B ₃	2981.4			
12		A	2981.0		2970.6 (A)	
13		B ₃	1483.1		1566.0 (B ₃)	
14		B ₁	1480.1	CH ₃ wagging +		
15	M4	B ₂	1479.2	NO ₂ antisymmetric stretching	1565.4 (B ₂)	1528
16		A	1456.3			
17		B ₁	1434.5			
18	M5	B ₃	1429.3	CH ₃ deformation +	1429.6 (B ₃)	
19		B ₂	1419.1	NO ₂ antisymmetric stretching	1430.9 (B ₂)	1434
20		A	1418.6			
21		B ₂	1406.9		1414.1 (B ₂)	
22		B ₁	1396.6	CH ₃ deformation +	1412.7 (B ₁)	
23	M6	B ₃	1384.1	NO ₂ symmetric stretching	1413.6 (B ₃)	1414
24		A	1381.3		1412.0 (A)	
25		B ₂	1371.4		1414.7 (B ₂)	
26	M7	B ₁	1368.2	CH ₃ deformation +		
27		B ₃	1360.6	NO ₂ symmetric stretching		1387
28		A	1356.0		1403.9 (A)	
29		B ₂	1310.3		1376.5 (B ₂)	
30	M8	B ₃	1310.1	CH ₃ wagging + NO ₂ stretching+	1378.2 (B ₃)	1342
31		B ₁	1308.2	CN stretching	1379.3 (B ₁)	
32		A	1307.9		1375.4 (A)	
33		B ₂	1095.4		1120.1 (B ₂)	
34	M9	B ₁	1090.5	NCH deformation	1121.2 (B ₁)	1098
35		B ₃	1089.5		1124.3 (B ₃)	
36		A	1088.3			
37		B ₃	1076.7		1108.2 (B ₃)	
38		A	1075.5	CH ₃ twisting +	1105.3 (A)	
39	M10	B ₂	1073.5	NO ₂ antisymmetric stretching	1107.1 (B ₂)	1083
40		B ₁	1070.7		1106.1 (B ₁)	
41		A	890.1		923.6 (A)	
42		B ₂	889.9	CN stretching +	923.8 (B ₂)	906
43	M11	B ₁	889.1	NO ₂ bending	922.0 (B ₁)	
44		B ₃	888.9			
45		B ₁	641.5		658.0 (B ₁)	
46	M12	B ₂	641.1	CN stretching +	664.4 (B ₂)	650
47		B ₃	641.0	NO ₂ scissor		
48		A	636.3			
49		B ₁	592.4		610.1(B ₁)	
50	M13	B ₂	591.4	NCH wagging +	608.0 (B ₂)	
51		B ₃	587.3	NO ₂ antisymmetric stretching	607.7 (B ₃)	601
52		A	585.9			
53		B ₂	472.7		484.1 (B ₂)	
54	M14	A	470.9		484.9 (A)	472
55		B ₃	470.6	NO ₂ rocking	484.0 (B ₃)	
56		B ₁	470.3		483.7 (B ₁)	

TABLE IV: Vibrational frequencies (in cm^{-1}) of the external modes of solid nitromethane. All quantities are calculated at the respective theoretical equilibrium volume using the GGA+G06 functional. Here A(R), B_1 (R+IR), B_2 (R+IR) and B_3 (R+IR) are irreducible representation of space group $P2_12_12_1$.

no.	Mode	Irr rep	Cal. fre	Exp ^s
57		A	180.9	
58		B_2	171.1	165.4(B_2)
59		B_1	162.0	
60	L1	B_3	161.4	
61		A	153.6	154.9(A)
62		B_2	148.5	
63		B_3	145.7	
64	L2	B_1	132.9	138.8(B_1)
65		B_3	116.1	114.6(B_3)
66		B_1	113.0	
67	L3	B_2	107.7	
68		A	106.3	112.9(A)
69		B_3	100.5	
70		B_2	97.6	95.1 (B_2)
71	L4	B_1	91.2	99.7(B_1)
72		B_3	90.5	85.0(B_3)
73		A	84.4	84.5(A)
74		B_1	73.1	78.2(B_1)
75		B_2	71.6	71.5(B_2)
76	L5	A	70.1	70.7(A)
77		A	66.1	58.6(A)
78		B_3	62.7	
79		A	53.7	52.1(A)
80	L6	B_2	51.8	44.4(B_2)
81		B_1	44.1	

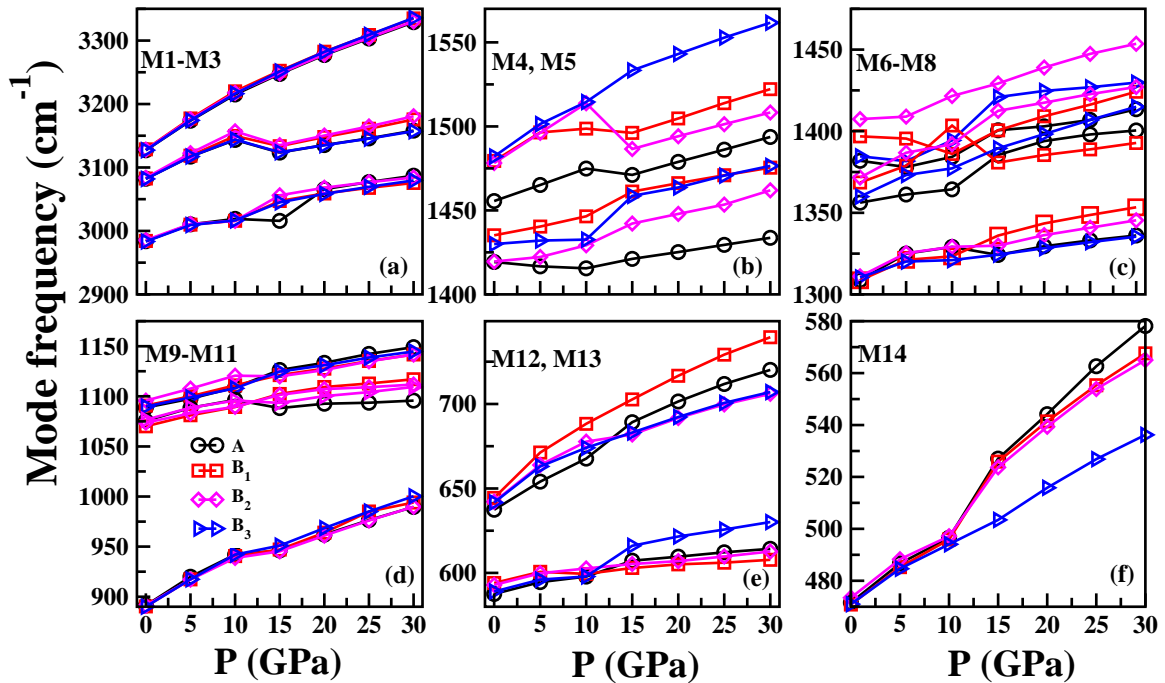


FIG. 6: (Colour online) Pressure evolution of internal vibrational frequencies of solid nitromethane up to 30 GPa using PBE-G06 at Gamma point.

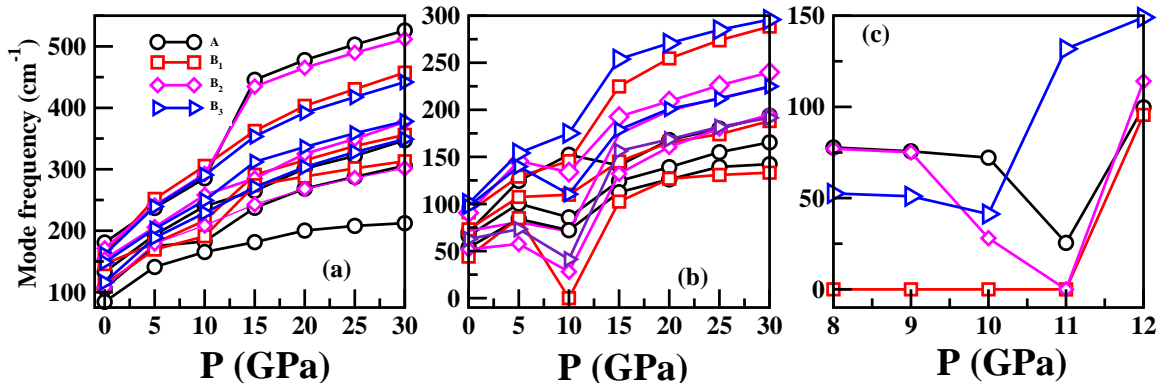


FIG. 7: (Colour online) Calculated L1-L3 (a), L4-L6 (b) external vibrational frequencies of solid nitromethane at Gamma point up to 30 GPa (step size of 5 GPa) within PBE-G06 and (c) shows the L6 mode frequencies from 8 GPa to 12 GPa with a step size of 1 GPa.

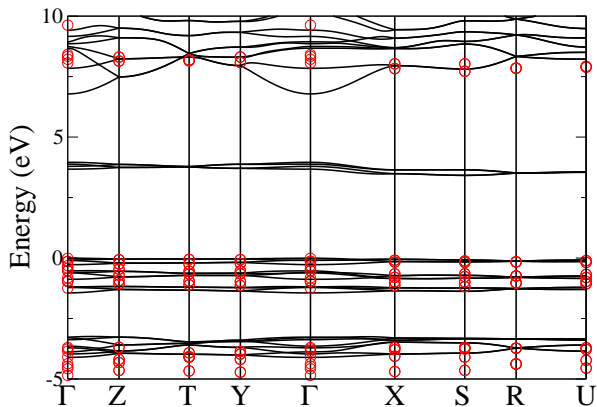


FIG. 8: (Color online) Band structure of solid nitromethane within GGA (black lines) and G₀W₀ approximation (red circles) at experimental lattice vectors.

sented in Fig 8 (solid lines). The top of the valence band and the bottom of the conduction band occur at the Γ and X high symmetry points respectively, and the magnitude of our GGA bandgap (3.8 eV) is in good agreement with the previously reported theoretical values of 3.61 eV¹⁶ and of 3.28 eV.⁵⁵ However band-gaps obtained using standard DFT functionals are usually underestimated when compared to experiments. To solve this problem, we have used the GW approximation to treat excited states as implemented in the VASP code using projector augmented waves method.⁵⁶ The calculated quasiparticle band structure of solid nitromethane is presented in Fig. 8 (red circles), where it is compared to its GGA counterpart (solid lines). Our calculated GW band gap value is 7.8 eV, which is a significant correction of the GGA value. As with the GGA, the band-gap is indirect from the Γ point to the X point. From the calculated band structure as shown in Fig 8, the valence band splits into

four distinct manifolds. The lower manifold that extends from about -3 eV to -4 eV is derived from the *p* states of C atoms and partly of *s* states of H atoms. The upper manifold that extends up to the Fermi level is mostly from the hybridization of *p* states of C and O atoms, respectively. The middle regions, that are -0.5 eV to -1.0 eV and -1.5 to -2 eV are due to the hybridization of C and O atoms. The conduction band is mainly dominated by the H-*s* states and from states of O and N atoms. Moreover, the important correction brought by the GW approximation in the case of nitromethane implies that the GGA values of the band gap usually used for other secondary explosives to predict their exact sensitive impact factor needs to be reinvestigated.

E. Optical properties

In this section, we focus on the optical properties of solid nitromethane. In general, the optical properties of matter can be described by means of the complex dielectric function $\epsilon(\omega) = \epsilon_1(\omega) + i\epsilon_2(\omega)$, where $\epsilon_1(\omega)$ and $\epsilon_2(\omega)$ describes the dispersive and absorptive parts of the dielectric function. Generally, there are two contributions to $\epsilon(\omega)$, namely the intraband and interband parts. The contribution of intraband transitions are important only for metals while the interband transitions can be split into direct and indirect transitions. We have neglected the indirect transitions involving scattering of phonons assuming that they give small contribution to $\epsilon(\omega)$ in comparison to direct transitions.⁵⁷ Then $\epsilon(q=0, \omega)$ is calculated using the random phase approximation without local field effects. In particular, the imaginary part is determined by a summation over empty states, and then the real part $\epsilon_1(\omega)$ of the dielectric function can be evaluated from $\epsilon_2(\omega)$ using Kramer-Kronig relations. The knowledge of the real and imaginary parts of the dielectric function allows the calculation of the important optical properties such as refractive index and absorption. Since, solid nitromethane crystallizes in an or-

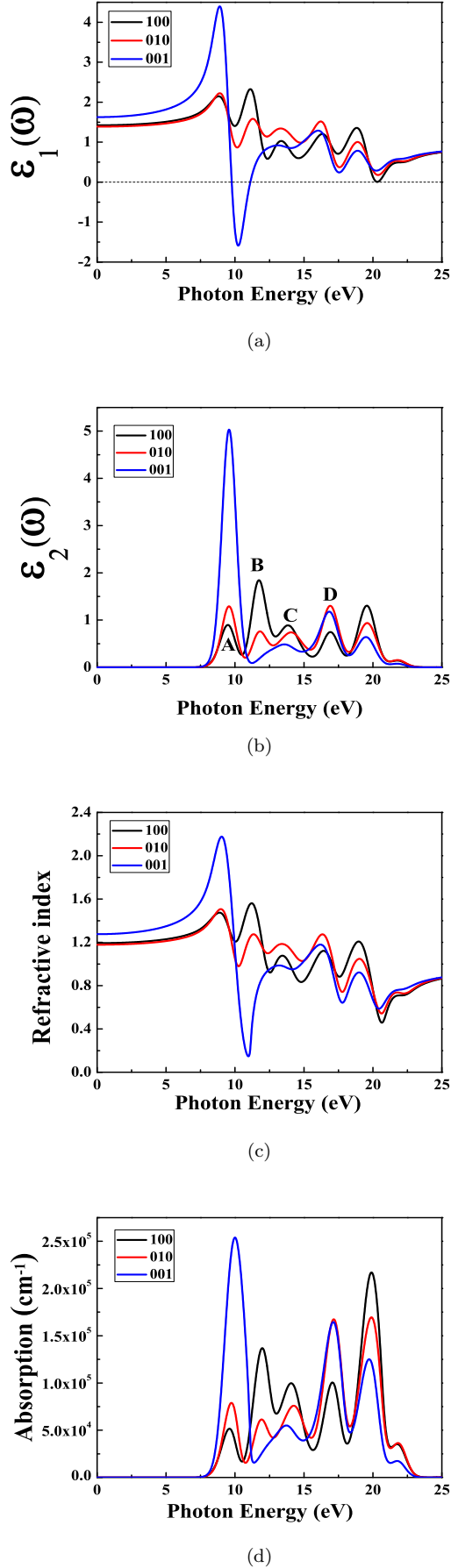


FIG. 9: (Color online) Optical properties of solid ni-

thorhombic structure, the optical functions are expected to be different along the three crystallographic directions [1 0 0], [0 1 0] and [0 0 1]. We have calculated the optical properties using the CASTEP code within GGA but a scissor shift of 4.6 eV is applied to the conduction bands to be consistent with the calculated value of the band gap obtained with the GW approximation.

Our calculated optical functions of solid nitromethane are presented in Figure 9 for an energy range up to 25 eV. The dispersive part of the dielectric function ($\epsilon_1(\omega)$) is shown in Fig 9 (a). The static dielectric function $\epsilon_1(0)$ of solid nitromethane along the three directions are found to be $\epsilon_1(0) = 1.42$ along the [1 0 0] direction, $\epsilon_1(0) = 1.39$ along the [0 1 0] direction and $\epsilon_1(0) = 1.63$ along the [0 0 1] direction. The absorptive part of the dielectric function ($\epsilon_2(\omega)$) is shown in Fig. 9(b). The main peaks in the [1 0 0] direction are marked as A (at 9.5 eV), B (at 11.7 eV), C (at 13.8 eV) and D (at 16.9 eV). A similar structure is observed in the case of [0 1 0] and [0 0 1] crystallographic directions albeit with a slight energy shift and different intensities. The peak A originates from transitions between O (p) and H (s) states for all the three crystallographic directions. The peak B arises from transitions of the C (p) states to the H (s) states along [1 0 0] and [0 1 0] directions, while it is absent for the [0 0 1] direction. The peak C along the three directions comes from transitions between the s states of O and the p states of C to the p states of N and O atoms. The peak D results from transition from C, N, O p states to O, N 2s states along the three crystallographic directions. Then from the calculated $\epsilon_1(\omega)$ and $\epsilon_2(\omega)$, we have evaluated the refractive index (n) and absorption shown in Fig. 9(c) and Fig. 9(d) respectively. The static refractive index $n(0)$ along three directions: $n(0) = 1.19$ along [1 0 0], $n(0) = 1.18$ along [0 1 0] and $n(0) = 1.27$ along [0 0 1]. In Fig 7(d), we show the calculated absorptive spectra along the three directions. The absorption starts at an energy of 7.8 eV which is the band gap, whereas the edge of absorption occurs at 9.60 eV along the [1 0 0] direction, at 9.77 eV along the [0 1 0] direction, and at 9.98 eV along the [0 0 1] direction. The related absorptive coefficients are found to be different along the three directions and are around $5 \times 10^4 \text{cm}^{-1}$ (along [1 0 0]), $7.8 \times 10^4 \text{cm}^{-1}$ (along [0 1 0]) and $2.5 \times 10^5 \text{cm}^{-1}$ (along [0 0 1]). From these results, it appears that solid nitromethane is an optically anisotropic material.

IV. CONCLUSIONS

In summary, we have investigated the structural properties of solid nitromethane within LDA and GGA with different functional including dispersion corrections to treat vdW forces. It was found that the structural properties using PBE-G06 are in good agreement with experiments, which highlight the role of vdW interactions in solid nitromethane. Then, the influence of hydrostatic pressure on the structural properties such as the lattice

parameters, the bond lengths, and the bond angles was calculated and a discontinuity in bond lengths and bond angles was observed between 10 GPa to 12 GPa. Also, we have estimated the elastic constants for this material using PBE-G06 and found that the material is mechanically stable. In particular, solid nitromethane is stiffest along the crystallographic a-axis, followed by the b-axis, and then by the c-axis. The vibrational properties of solid nitromethane at ambient conditions have been calculated and a fairly good agreement with experiments was reported. The influence of hydrostatic pressure on solid nitromethane shows distinct behavior from 8 to 15 GPa. From the weakening of hydrogen bond strength, softening of lattice modes supports a possible structural transition in solid nitromethane between 8 to 12 GPa and this was in excellent agreement with reported experiments. Finally, we have used the GW approximation to obtain an accurate value of the band gap and presented the corresponding quasiparticle band structure. We found that

nitromethane has an indirect band gap of approximately 7.8 eV which occurs between the high symmetry points Γ and X. The calculated dielectric function, refractive index, and absorption functions along three crystallographic directions shows a considerable anisotropy. We expect that our results will stimulate further experiments on solid nitromethane but also that they will be useful to understand other materials used as explosives.

V. ACKNOWLEDGMENTS

S. A. would like to thank DRDO through ACRHEM for financial support and thank CMSD, University of Hyderabad, for providing computational facilities. S. L acknowledges GENCI-CCRT/CINES (Grant x2013-085106) for access to computational facilities. **Author for Correspondence, E-mail: gvaithee@gmail.com*

-
- ¹ S. F. Trevino, E. Prince, C. R. Hubbard, J. Chem. Phys. **73**, 2996 (1980).
 - ² J. M. Seminario, M. C. Concha, and P. Politzer, J. Chem. Phys. **102**, 8281 (1995).
 - ³ Don T. Cromer, Robert R. Ryan and David schifel, J. Phys. Chem. **89**, 2315-2318 (1985).
 - ⁴ F. L. Yarger, B. Olinger J. Chem. Phys. **85**, 1534 (1986).
 - ⁵ Margherita Citroni, frederic Datchi, Roberto Bini, Massimo Di Vaira, Philippe Pruzan, Bernard Canny and Vincenzo Schettino, J. Phys. Chem. B **112**, 1095-1103 (2008).
 - ⁶ P. J. Miller, S. Block, G. J. Piermarini, J. Phys. Chem. **93**, 462-466 (1989).
 - ⁷ J. R. Hill, D. S. Moore, S. C. Schmidt and C. B. Strom J. Phys. Chem **95**, 3037-3044 (1991).
 - ⁸ R. Ouillon, J.-P. Pinan-Lucarre, P. Ranson, G. Baranovic, J. Chem. Phys **116**, 4611 (2002).
 - ⁹ J.-P. Pinan-Lucarre, R. Ouillon, B. Canny, Ph. Pruzan, P. Ranson, Journal of Raman Spectroscopy **34**, 819 (2003).
 - ¹⁰ R. Ouillon, J.-P. Pinan-Lucarre, B. Canny, Ph. Pruzan, P. Ranson, Journal of Raman Spectroscopy **39**, 354 (2008).
 - ¹¹ D. C. Sorescu, B. M. Rice, and D. L. Thompson, J. Phys. Chem. B **104**, 8406 (2000).
 - ¹² D. C. Sorescu, B. M. Rice, and D. L. Thompson, J. Phys. Chem. A **105**, 9336 (2001).
 - ¹³ P. M. Agarwal, B. M. Rice, and D. L. Thompson, J. Chem. Phys. **119**, 9617 (2003).
 - ¹⁴ E. F. C. Byrd, G. E. Scuseria, C. F. Chabalowski, J. Phys. Chem. B **108**, 13100 (2004).
 - ¹⁵ E. J. Reed, J. D. Joannopoulos, and L. E. Fried, Phys. Rev. B **62**, 16500 (2000).
 - ¹⁶ H. Liu, J. Zhao, D. Wei, and Z. Gong, J. Chem. Phys. **124**, 124501 (2006).
 - ¹⁷ Frank J. Zerilli, Joseph P. Hooper, Maija M. Kuklja, J. Chem. Phys **126**, 114701 (2007).
 - ¹⁸ Mark E. Tuckerman, Micheale Klein, Chemical Physics Letters **283**, 147-151 (1998)
 - ¹⁹ H. E. Alper, F. A. Awwad and P. Poltizer, J. Phys. Chem B **103**, 9738-9742 (1999).
 - ²⁰ M. Riad Manna, Evan J. Reed, Laurence E. Fried, Giulia Galli and Francois Gygi J. Chem. Phys **120**, 10146-10153 (2004).
 - ²¹ J. Chang, P. Lian, D. Q. Wei, X. R. Chen, Q. M. Zhang, Z. Z. Gong, Phys. Rev. Lett. **105**, 188302 (2010).
 - ²² D. C. Sorescu, B. M. Rice, J. Phys. Chem C **114**. 6734-6748 (2010).
 - ²³ A. C. Landerville, M. W. Conroy, M. M. Budzevich, Y. Lin, C. T. White, I. I. Oleynik, Appl. Phys. Lett **97**, 251908 (2010).
 - ²⁴ S. Grimme, J. Comp. Chem. **27**, 1787 (2006).
 - ²⁵ A. Neumann and M.-A. Perrin, J. Phys. Chem. B **109**, 15531 (2005).
 - ²⁶ Weihua Zhu, Heming Ziao , Struct Chem **21**, 657-655 (2010).
 - ²⁷ John P. Perdew, Mel Levy, Phys. Rev. Lett **51**, 1884-1887 (1983).
 - ²⁸ R. O. Jones, O. Gunnarsson, Rev. Mod. Phys **61**, 689-746 (1989).
 - ²⁹ S. Lebègue, B. Arnaud, M. Alouani, P. E. Blöchl, Phys. Rev. B **67**, 155208 (2003).
 - ³⁰ S. Lebègue, B. Arnaud, and M. Alouani, Phys. Rev. B **72**, 085103 (2005).
 - ³¹ M. W. Conroy, I. I. Oleynik, S. V. Zybin, C. T. White, J. Phys. Chem. A **113**, 3610-3614 (2009).
 - ³² W. Kohn, L. J. Sham, Phys. Rev. **140**, A1133 (1965).
 - ³³ M. C. Payne, M. P. Teter, D. C. Allan, T. A. Arias and J. D. Joannopoulos, Rev. Mod. Phys. **64**, 1045 (1992).
 - ³⁴ M. D. Segall, P. J. D. Lindan, M. J. Probert, C. J. Pickard, P. J. Hasnip, S. J. Clark and M. C. Payne, J. Phys. Cond. Matt. **14**, 2717 (2002).
 - ³⁵ D. M. Ceperley and B. J. Alder, Phys. Rev. Lett. **45**, 566 (1980).
 - ³⁶ J. P. Perdew and A. Zunger, Phys. Rev. B **23**, 5048 (1981).
 - ³⁷ J. P. Perdew and Y. Wang, Phys. Rev. B **45**, 13244 (1992).
 - ³⁸ J. P. Perdew, K. Burke and M. Ernzerhof, Phys. Rev. Lett. **77**, 3865 (1996).
 - ³⁹ H. J. Monkhorst and J. Pack, Phys. Rev. B **13**, 5188 (1976).
 - ⁴⁰ D. Vanderbilt, Phys. Rev. B **41**, 7892 (1990).

- ⁴¹ F. Ortmann, F. Bechstedt and W. G. Schmidt, Phys. Rev. B **73**, 205101 (2006).
- ⁴² A. Tkatchenko and M. Scheffler, Phys. Rev. Lett. **102**, 073005 (2009).
- ⁴³ O. Gunnarsson, K. Schonhammer, Phys. Rev. Lett **56** 1968 - 1971 (1986).
- ⁴⁴ L. Hedin, Phys. Rev. **139** A796 (1965).
- ⁴⁵ L. Hedin and S. Lundquist, Solid State Physics, edited by H. Ehrenreich, F. Seitz, and D. Turnbull, vol 23, Academic, New York (1969).
- ⁴⁶ N. V. Smith , Phys. Rev. B **3**, 1862 (1971).
- ⁴⁷ H. Ehrenreich, M. H. Cohen, Phys. Rev **115**, 786 (1959).
- ⁴⁸ G. Onida, L. Reining, A. Rubio, Rev. Mod. Phys. **74**, 601 (2002).
- ⁴⁹ G. Kresse, J. Furthmuller, Phys. Rev. B **54**, 11169 (1996).
- ⁵⁰ M.J. Mehl, J.E. Osburn, D.A. Papaconstantopoulos, B.M. Klein, Phys. Rev. B **41**, 10311 (1990).
- ⁵¹ M. Born, K. Huang, Dynamical Theory of Crystal Lattices (Oxford: Oxford University Press)(1998).
- ⁵² James J. Haycraft, Lewis L. Stevens, Craig J. Eckhardt J. Chem. Phys. **124**, 024712 (2006)
- ⁵³ Lewis L. Stevens, Craig J. Eckhardt J. Chem. Phys. **122**, 174701 (2005)
- ⁵⁴ J. M. Winey, Y. M. Gupta, J. Appl. Phys. **90**, 1669 (2001).
- ⁵⁵ M. R. Manaa, E. J. Reed, L. E. Fried, J. Chem. Phys. **98**, 10146 2004.
- ⁵⁶ P. E. Blöchl, Phys. Rev. B **50**, 17953 1994.
- ⁵⁷ N. V. Smith, Phys. Rev. B. **3**, 1862 (1971).
- ⁵⁸ H. Ehrenreich, M. H. Cohen, Phys. Rev. **115**, 786 (1959).